SAND2011-2811C

# On the use of single-film models to describe the oxy-fuel combustion of pulverized coal char

Manfred Geier[1,*], Christopher R. Shaddix[1],
Kevin Davis[2], and Hong Shig-Shim[2]

[1]*Combustion Research Facility, Sandia National Laboratories, Livermore, CA 94550, USA*
[2]*Reaction Engineering International, Salt Lake City, UT USA*

CFD simulations traditionally rely on the computational efficiency of single-film global kinetic oxidation models to predict char particle temperatures and char conversion rates in pulverized coal boilers. In oxy-fuel combustion with flue gas recirculation (FGR), as is commonly employed, char combustion occurs in the presence of elevated $CO_2$ levels and, frequently, elevated water vapor levels (when employing wet FGR). Furthermore, local oxygen concentrations can be quite high in the vicinity of oxygen injection lances. The suitability of existing approaches to modeling char combustion under these conditions has been unclear. In particular, our previous work comparing experimental measurements of pc char combustion temperatures against detailed modeling of char combustion showed that both boundary layer conversion of CO and gasification reactions of steam and $CO_2$ need to be included to give reasonable agreement with the experimental measurements. In this study, we have developed an extended single-film reaction model that includes gasification reactions and systematically interrogated the performance of the model in comparison to experimental data for a Powder River Basin subbituminous coal and a low-sulfur high-volatile bituminous coal for a variety of model assumptions. While the extended single-film model cannot give ideal agreement with the data, reasonably good agreement is given for high temperature environments with 12-36 vol-% $O_2$ and 16 vol-% $H_2O$ in either $N_2$ or $CO_2$ diluent. To achieve such agreement with the data while maintaining reasonable values for activation energy of the reactions, incorporation of both steam and $CO_2$ gasification reactions is required.

## 1. Introduction

Coal combustion using pure oxygen as the oxidizer appears to be an economically promising process for $CO_2$ separation for carbon capture and storage and has thus received considerable attention of the scientific community in recent years (e.g. [1-3] and references therein). Flue gas recycling necessary for thermal control and material safety issues yields elevated concentrations of carbon dioxide and possibly also higher moisture contents in the char combustion environment. Retrofitted boilers typically have to be operated at enhanced oxygen levels to maintain similar heat transfer rates [4,5]. Furthermore, pure oxygen injection is typically employed with lances in oxy-fuel burners to aid flame attachment and stabilization [6-8], leading to locally high concentrations of oxygen.

Computational fluid dynamics (CFD) simulations have become an indispensable tool in design and optimization of coal-fired burners and boilers. High computational complexity dictates fairly coarse meshes for the spatial domain and application of simplified coal combustion models, which inevitably reduces the range of process conditions for which the simulation software produces reliable results. The char combustion process is commonly described through a single heterogeneous reaction, namely $C(s) + O_2 \rightarrow CO_2$ or by $C(s) + 1/2\ O_2 \rightarrow CO$ (sometimes including a rule to account for heat release by the oxidation of CO to $CO_2$ in the gas phase). Appropriate rate parameters

* Corresponding author. Fax. +1-925-294-2276
E-Mail address: mgeier@sandia.gov

for these simplistic kinetics models have been established empirically for conventional, air-blown combustion systems. When these parameters are used for the vastly different oxy-combustion environments, char burnout characteristics may be poorly predicted. In order to establish better char burnout models, it is necessary to understand the governing phenomena and their relevance for these unconventional combustion conditions.

Recent computational results suggest that the partial conversion of CO to $CO_2$ in the particle boundary layer has an important influence on the char particle temperatures and burning rates under oxygen-enriched combustion conditions [9,10]. In addition, char surface reactions with both steam and $CO_2$ could play an important role in the char oxidation process [10-12]. The highly endothermic char gasification reactions $C(s) + CO_2 \rightarrow 2CO$ and $C(s) + H_2O \rightarrow H_2 + CO$ have been found to reduce the temperature of pulverized coal chars burning at high temperatures in oxy-combustion environments, and to slightly enhance or reduce overall consumption rates depending on particle size and $O_2$ concentration [10,11].

The simulation code SKIPPY (Surface Kinetics in Porous Particles) [13], which calculates 1-D, steady-state species concentration and temperature profiles of a single, porous, spherical particle placed in a quiescent, chemically reacting environment, allows numerical investigation of the char consumption process to a high level of detail and serves as a heuristic tool to advance the understanding and guide further experimental investigations. Applied in this sense, SKIPPY predictions of temperatures of 100 µm particles have shown good agreement with experimental data when both steam and $CO_2$ gasification reactions were included [12]. The results indicate that a full mechanistic view of the char consumption process in oxy-combustion systems must consider steam and $CO_2$ gasification reactions, as well as CO conversion in the particle boundary layer. In order to assure CFD simulations produce reliable predictions for oxy-combustion systems, CFD codes must therefore account for these reactions (but under the constraint of sufficiently low computational cost).

In this study we explore a modification of the traditional single-film char burnout model (i.e. a model without gas-phase reactions and only char reaction with $O_2$) for that purpose. In particular, we consider augmenting the heterogeneous reaction mechanism with two (global) gasification reactions. In light of the aforementioned findings and the simplicity of the overall reaction mechanism, it is clear that the model is probably a poor representation of the actual chemical reaction mechanism, but the question is whether it can be useful for reliable predictions of char temperatures (and thus radiant heat transfer) and char conversion in CFD simulations. Evaluation of this extended single-film model with respect to the details of implementation and efficiency of the algorithm are beyond the scope of this paper. Rather, we focus here only on the model performance in predicting experimentally observable data (particle temperature) of char particles burning in $N_2$ and $CO_2$ baths with different contents of $O_2$. Predictions from models of different complexity and the values of the fitting parameters are used to assess model quality.

## 2. Experiment

The experimental data used consist of simultaneously measured size-temperature pairs of individual particles burning in isolation from each other. These data were obtained using an optical entrained flow reactor in a configuration schematically depicted in Figure 1 and described in more detail in [14]. The combustion-driven reactor relies on a diffusion-flamelet-based Hencken burner to produce a high-temperature gas flow at ambient pressure (1 atm) into which coal particles are introduced at the furnace centerline. The particle carrier flow rate is very small relative to the overall burner flow rate and compositionally matches the diluent in the main reactant flow (i.e. $N_2$ or $CO_2$). For the experimental results shown below the coal particles were delivered to the flow reactor at a rate sufficiently small (~0.6 g/hr) to assure that injected particles burned in isolation from one another. The hot, post-combustion gas flow is shielded from the surrounding air by means of a 46 cm tall 5 cm × 5 cm quartz chimney, which also provides optical access for *in situ* optical measurements on particles injected into the flow.

For comparisons with predictions of different char combustion models, size-classified coal par-

ticles were entrained into mixtures with 12, 24 or 36 mole-% $O_2$, 16% moisture, and $CO_2$ or $N_2$ as balance gas. Particle temperature-size data were collected at locations between 25 and 125 mm above the burner face. At these locations, the gas temperatures were 1680±40 K, with a peak at about 1700±10 K at 50 mm above the burner surface and a subsequent linear decay with height in the furnace [12]. The total burner product flow rate was 60 slpm (standard liters per minute), which includes 0.03 slpm of diluent flow for conveying the particles through the feed tube (0.75 mm ID).

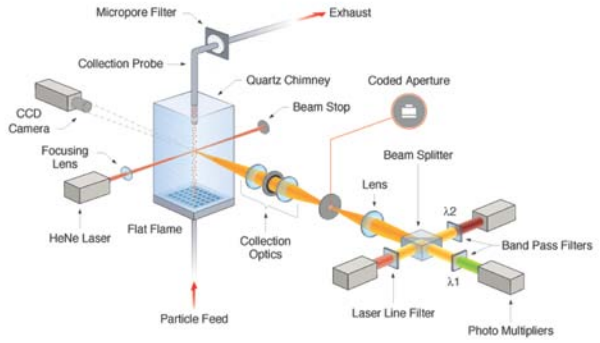


Fig. 1. Schematic of Sandia's laminar entrained flow reactor for coal combustion studies. The particle-sizing pyrometry diagnostic is shown to the right of the flow reactor.

The experimental data shown are for a western U.S., low-sulfur, high-volatile bituminous coal (Utah Skyline) and a low-sulfur subbituminous coal from the Powder River Basin (North Antelope), with proximate and ultimate analyses shown in Table 1. Analysis of three coal size fractions (53-75 µm, 75-106 µm and 106-125 µm) confirmed size-independent elemental composition and ash contents. The data presented here correspond to a coal particle feed of 75-106 µm.

## 3. Extended Single Film Model

Establishment of a model to account for gasification reactions on the char surface, in addition to the oxidation reaction, relies on the same simplifying assumptions used in the derivation of the single-film model as outlined e.g. in [15]. In essence, an instantaneous energy balance and equation for conservation of mass are formulated on a homogeneous, non-porous, chemically reacting, spherical particle with reactant species diffusing from an infinite boundary to the particle surface. As no reactions are assumed to take place in the gas phase, the location of species conversion occurs only on the char surface and is based on the following heterogeneous reactions:

$$C(s) + (1+\psi)/2\ O_2 \rightarrow \psi\ CO_2 + (1-\psi)\ CO \quad (1)$$

$$C(s) + CO_2 \rightarrow 2CO \quad (2)$$

$$C(s) + H_2O \rightarrow H_2 + CO \quad (3)$$

The $CO_2/CO$ production ratio is modeled as $CO_2/CO \equiv \psi/(1-\psi) = 0.02\, p(O_{2,s})^{0.21} \exp(3070/T)$ [16], where $p(O_{2,s})$ is the oxygen partial pressure at the particle surface in atm, and $T$ is the particle surface temperature. The carbon production rate in kmol/(m$^2$·s) follows from for an "$n$th-order" Arrhenius kinetics rate law for each reactant according to

$$\dot{s}''_{C(s)} = -A_i T^{b_i} \exp\left(-\frac{E_i}{RT}\right)\left[R_{i,s}\right]^{n_i}$$

where $[R_{i,s}]$ is the molar concentration of reactant $R_i = \{O_2, CO_2, H_2O\}$ at the particle surface in kmol/m$^3$, $E_i$ is the activation energy in kJ/mol, and universal gas constant $R = 8.3145$ J/(K·mol). Reaction orders of 1 ($n_i = 1$) are frequently employed in CFD codes for these reactions, a choice justifiable mainly on numerical rather than physical grounds (according to classical Thiele analysis, apparent reaction orders are constrained to lie

Table 1 Proximate and Ultimate Analysis of Coals

| | Coal Type | | | |
|---|---|---|---|---|
| | Utah Skyline | | North Antelope | |
| Proximate | wt%, as rec'd | wt% dry | wt%, as rec'd | wt% dry |
| moisture | 3.18 | | 23.69 | |
| ash | 8.83 | 9.12 | 4.94 | 6.47 |
| volatiles | 38.60 | 39.87 | 33.36 | 43.72 |
| fixed C | 49.39 | 51.01 | 38.01 | 49.81 |
| Ultimate | wt% dry | wt% DAF | wt% dry | wt% DAF |
| C | 70.60 | 77.44 | 53.72 | 56.51 |
| H | 5.41 | 5.93 | 6.22 | 6.54 |
| O (by diff.) | 13.21 | 14.49 | 34.11 | 35.88 |
| N | 1.42 | 1.56 | 0.78 | 0.82 |
| S | 0.53 | 0.58 | 0.23 | 0.24 |

between 0.5 and 1 for Zone II combustion with partial reactant penetration of the porous char [17, 18]). To follow the customary use of expressing the rate law in terms of reactant partial pressure instead of molar concentration, the temperature exponent $b_i = 1$. With these assumptions, the pre-exponential factors $A_i$ are given in units of m/s.

The energy balance for steady-state consumption of char according to reactions 1-3 assumes the same form as for the traditional single-film model [12,19], but with additional expressions for gas properties and overall heat of reaction. As $CO_2$ is both a reactant and a product species, the differential equations for species conservation are somewhat more involved, but can still be solved analytically as long as constant gas properties are assumed. Due to reaction coupling through the individual char consumption rates, a solver for systems of nonlinear equations is generally necessary, however. While information on gas properties and other required input parameters can be readily obtained, kinetics rate parameters must be found empirically by fitting the model to the experimental data. For the limited amount of data at hand, typical literature values are substituted for the gasification activation energies here, leaving at most four parameters for the fit. The obtained rate parameters for the models discussed below are summarized in Tables 2 and 3, with numerical subscripts 1-3 referring to reactions 1-3.

## 4. Results and Discussion

Figure 2 shows the measured char particle temperature data for Utah Skyline char particles burning in $N_2$ (left) and $CO_2$ (right) diluents together with best-fit single-film model predictions corresponding to the rate parameters shown in Table 2. Consistent with the findings in [9], measured temperatures are, for comparable $O_2$ concentrations, on average lower in the $CO_2$ environment. The data suggest that particle temperatures are nearly independent of particle size, with a mild negative correlation with size for lower oxygen concentrations. The data show an average char particle size of ~ 100 µm (consistent with the coal feed range of 75-106 µm), so temperature data for the reported sizes between 97 and 103 µm are therefore used to fit the models. To properly balance the model fits to variations in particle temperature (as the $O_2$ content in the gas is varied) and to the presence or absence of significant $CO_2$ concentrations, the different models shown in Tables 2 and 3 were adjusted manually to best match data for 12% and 36% $O_2$ in $N_2$ and 36% $O_2$ in $CO_2$ bath gas.

The best-fit results for a traditional oxidation-only model (Model I, not shown here) cannot predict the data well for both $N_2$ and $CO_2$ environments, and the obtained best-fit activation energies are zero or even negative, clearly in discord with physically reasonable values, indicating model inadequacy. These results have been previously reported [20]. Fig. 2 shows the best-fit single-film model results when including gasification

Table 2 Rate parameters for Utah Skyline char conversion

| Model | $A_1$ m/s | $E_1$ kJ/mol | $A_2$ m/s | $E_2$ kJ/mol | $A_3$ m/s | $E_3$ kJ/mol |
|---|---|---|---|---|---|---|
| II | 0.0146 | 1.5 | 300 | 251.0 | 0 | 0 |
| IIIa | 0.0334 | 13.9 | 340 | 251.0 | 100 | 221.8 |
| IIIb | 0.0981 | 29.4 | 390 | 251.0 | 300 | 221.8 |
| IIIc | 0.499 | 50.6 | 440 | 251.0 | 1000 | 221.8 |

Table 3 Rate parameters for North Antelope char conversion

| Model | $A_1$ m/s | $E_1$ kJ/mol | $A_2$ m/s | $E_2$ kJ/mol | $A_3$ m/s | $E_3$ kJ/mol |
|---|---|---|---|---|---|---|
| II | 0.0278 | 3.6 | 500 | 251.0 | 0 | 0 |
| IIIa | 0.116 | 25.5 | 590 | 251.0 | 100 | 221.8 |
| IIIb | 0.751 | 53.3 | 680 | 251.0 | 300 | 221.8 |
| IIIc | 22.2 | 99.4 | 740 | 251.0 | 1000 | 221.8 |

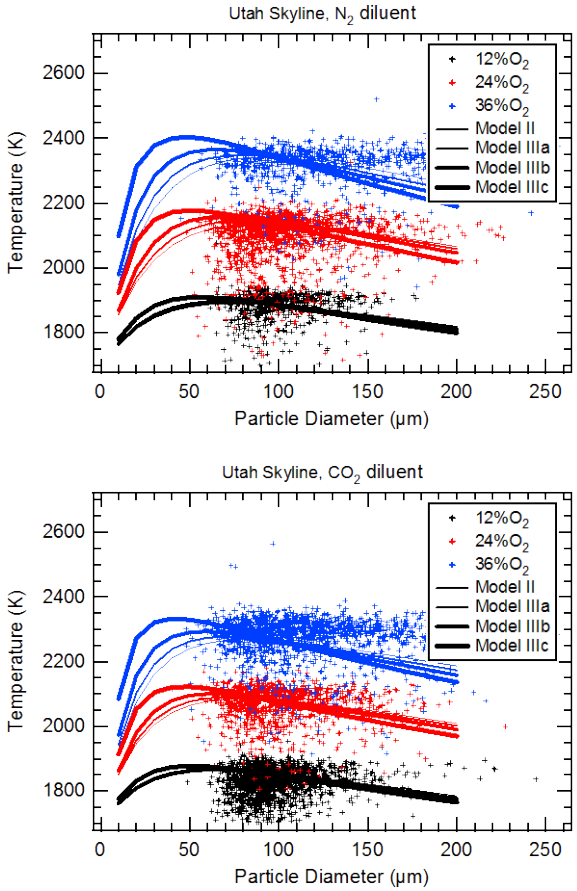


Fig. 2. Predicted and measured (symbols) Utah Skyline char particle temperatures for three free-stream $O_2$ concentrations, 16% moisture, and $N_2$ and $CO_2$ bath gas. Curves are predictions by models that allow for char consumption through oxidation and both steam and $CO_2$ gasification. Models IIIa-c refer to different pre-exponential factors for the steam gasification reaction (Table 2).

reactions. Model II includes char gasification by $CO_2$, but ignores steam gasification. This model, with three fitting parameters (a typical value 251 kJ/mol [12] was assumed for the activation energy of the gasification reaction), can, as expected, predict the temperatures around the fitting particle size 100 µm and gives reasonable fits for both $N_2$ and $CO_2$-dominated environments. However, the value of the apparent activation energy of the oxidation reaction is physically unrealistic and thus indicative of model inadequacy. As 16% moisture was present in the test environments, it is possible that steam gasification plays a role in determining the char particle temperature. In that case, CFD model predictions may rapidly lose their validity at other levels of moisture when Model II is used.

Figure 2 also shows the prediction results for Model III, when including the steam gasification reaction together with $CO_2$ gasification. Results for submodels a-c of Model III correspond to different assumed values of the pre-exponential factor $A_3$ of the steam gasification reaction, while holding the activation energy fixed at 222 kJ/mol [11]. Obviously, models with $A_3$ between 0 and 1000 m/s can all be reasonably fitted to the 100 µm data, which is no surprise given the constant moisture level for all data. A unique solution would require matching to data over a wide range of steam levels. Another means of differentiating the results for different assumed values of the steam gasification rate is to compare the derived best-fit apparent char oxidation activation energies. As shown in Table 2, the best-fit apparent activation energy for the oxidation reaction varies between 14 and 51 kJ/mol. These are rather low values, but with an $A_3$ value of 1000 m/s at least we are approaching the expected Zone II char oxidation $E_a$ of ~ 80 kJ/mol [21]. The best-fit char oxidation activation energy may be low because the assumption $n_{O_2} = 1$ may be too large. While frequently used in CFD codes, this assumption has been questioned by the scientific community [22]. Alternatively, Langmuir kinetics models have been proposed as being more appropriate than power-law kinetics models, at least for steam and $CO_2$ gasification reactions. Another reason for unrealistically low oxidation activation energies, however, is the likely relevance of CO conversion in the boundary layer (as suggested by our previous detailed modeling), which is ignored in the single-film models discussed here. Note that we have also performed fits with lower presumed activation energies of the two gasification reactions, corresponding to Zone II behavior for those reactions, but this yields even lower values of the derived activation energy of the oxidation reaction.

Figure 3 shows experimental data and model predictions for North Antelope char particles. These particles burn hotter than the Utah Skyline particles, corresponding to their higher reactivity

(as expected for a lower rank coal). The trends in both the data and the model fits are similar to those previously described for the Utah Skyline coal, except that the best-fit oxidation activation energies are somewhat higher. In particular, an apparent activation energy of 53 kJ/mol is obtained for the oxidation reaction when a steam gasification pre-exponential of 300 m/s is used. Therefore, for best self-consistency in the temperature dependence of char oxidation, we recommend using the model parameters highlighted in yellow in Tables 2 and 3.

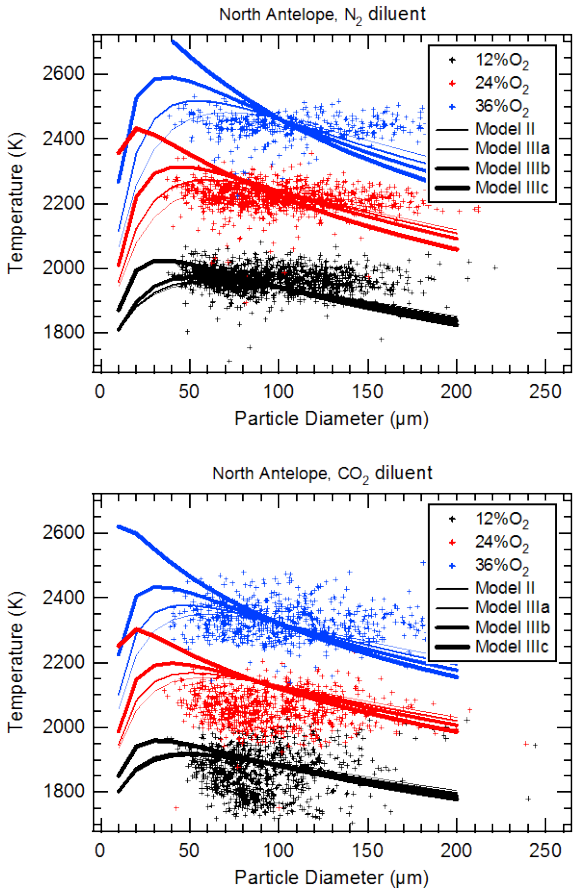


Fig. 3. Predicted and measured (symbols) Utah Skyline char particle temperatures for three free-stream $O_2$ concentrations, 16% moisture, and $N_2$ and $CO_2$ bath gas. Curves are predictions by models that allow for char consumption through oxidation and both steam and $CO_2$ gasification. Models IIIa-c refer to different pre-exponential factors for the steam gasification reaction (Table 2).

## 5. Summary

The traditional single-film *n*th-order Arrhenius char oxidation model was extended by including additional heterogeneous reactions of char with $CO_2$ and $H_2O$, as is required to accurately predict char particle temperatures and char consumption rates in both conventional and oxy-combustion environments. Particle temperatures from two-color pyrometer measurements of char particles burning in $N_2$ and $CO_2$ dominated gas environments were compared with predictions from the developed models with the goal to assess their predictive performance as part of CFD software. The results suggest that char consumption characteristics can be predicted reasonably well with the extended single-film model for a wide range of $O_2$ and $CO_2$ concentrations. Despite the wide application range, however, best-fit values of kinetic parameters are somewhat outside the range of physical meaningfulness, likely reflecting limitations from the neglect of CO conversion in the boundary layer, varying penetration of reactants into the char particle, and uncertainties in the actual heterogeneous reaction mechanism.


## Acknowledgement

This research was sponsored by the U.S. Department of Energy's Carbon Sequestration Program under award number DE-NT0005288. This work is part of a project led by Reaction Engineering International and is managed by Mr. Timothy Fout of the National Energy Technology Laboratory. Sandia is a multiprogram laboratory operated by Sandia Corporation, a Lockheed Martin Company, for the United States Department of Energy's National Nuclear Security Administration under Contract DE-AC04-94AL85000.




## References


[1] B.J.P. Buhre, L.K. Elliott, C.D. Sheng, R.P. Gupta, T.F. Wall, *Prog. Energy Combust. Sci.* 31 (4) (2005) 283-307.

[2] R. Tan, G. Corragio, S. Santos, *Oxy-Coal combustion with flue gas recycle for the power generation industry. A literature review*, Report No. IFRF Doc. No. G 23/y/1, International Flame Research Foundation, 2005.
[3] M.B. Toftegaard, J. Brix, P.A. Jensen, P. Glarborg, A.D. Jensen, *Prog. Energy Combust. Sci.* 36 (2010) 581-625.
[4] R. Payne, S.L. Chen, A.M. Wolsky, W.F. Richter, *Combust. Flame* 67 (1989) 1-16.
[5] H. Liu, R. Zailani, B.M. Gibbs, *Fuel* 84 (16) (2005) 2109-2115.
[6] N. Kimura, K. Omata, T. Kiga, S. Takano, S. Shikisima, *Energy Convers. Mgmt.* 36 (1995) 805-808.
[7] E. Croiset, K.V. Thambimuthu, A. Palmer, *Can. J. Chem. Eng.* 78 (2000) 402-407.
[8] J. Shan, A. Fry, *Oxy-coal burner design for utility boilers*, in Oxy-fuel combustion for power generation and carbon dioxide ($CO_2$) capture, (L. Zheng, Ed.), Woodhead Publishing, Oxford, 2011.
[9] C.R. Shaddix, A. Molina, *Effect of $O_2$ and High $CO_2$ Concentrations on PC Char Burning Rates during Oxy-Fuel Combustion*, Proceedings of the 33rd International Technical Conference on Coal Utilization and Fuel Systems, Clearwater, FL, June 1-5, 2008.
[10] E. S. Hecht, C. R. Shaddix, A. Molina, B. S. Haynes *Proc. Combust. Inst.* 33 (2011) 1699-1706.
[11] C.R. Shaddix, E.S. Hecht, M. Geier, A. Molina, B.S. Haynes, *Effect of gasification reactions on oxy-fuel combustion of pulverized coal char*, Proceedings of the 35th International Technical Conference on Clean Coal & Fuel Systems, Clearwater FL, June 6–10, 2010.
[12] M. Geier, C.R. Shaddix, B.S. Haynes, *27th Annual International Pittsburgh Coal Conference, Istanbul, Turkey, Oct. 11-14, 2010*
[13] P.J. Ashman, B.S. Haynes, *Improved techniques for the prediction of NOx formation from char nitrogen*, Project No. C4065, Australian Coal Association. CSIRO Energy Technology, 1999.
[14] D.A. Tichenor, S. Niksa, K.R. Hencken, R.E. Mitchell, *Proc. Combust. Inst.* 20 (1984) 1213-1221.
[15] S.R. Turns, *An Introduction to Combustion: Concepts and Applications*, McGraw-Hill, New York, (1996)
[16] L. Tognotti, J.P. Longwell, A.F.Sarofim, *Proc. Combust. Inst.* 23 (1990) 1207-1213.
[17] E.W. Thiele, *Ind. Eng. Chem.* 31 (1939) 916–920.
[18] M.F.R. Mulcahy, I.W. Smith, *Rev. Pure. Appl. Chem.* 19 (1969) 81–108.
[19] J.J. Murphy, C.R. Shaddix, *Combust. Flame* 144 (2006) 710-729.
[20] M. Geier, C.R. Shaddix, *A Modified Single-Film Char Consumption Model for CFD Simulations of Oxy-Combustion of Pulverized Coal*, 7th U.S. National Combustion Meeting, paper 2F07, Atlanta, GA, March 20-23, 2011.
[21] R.H. Hurt, J.K. Sun, M. Lunden, *Combust. Flame* 113 (1998) 181-197.
[22] R.H. Hurt, J.M. Calo, *Combust. Flame* 125 (2001) 1138-1149.